SEPTEMBER 1978 LRP 148/78

SPECTRAL ANALYSER FOR THOMSON SCATTERING

A.W. DeSilva*

*University of Maryland, College Park, Md.20742, USA;

Centre de Recherches en Physique des Plasmas

ECOLE POLYTECHNIQUE FEDERALE DE LAUSANNE

SPECTRAL ANALYSER FOR THOMSON SCATTERING

A.W. DeSilva

Centre de Recherches en Physique des Plasmas
Ecole Polytechnique Fédérale de Lausanne
CH-1007 Lausanne / Switzerland

Abstract

We describe here a four-channel spectral analyser suitable for use in Thomson scattering diagnostics of plasmas, that incorporates several novel features and is inexpensive and physically compact. It is suitable for spectral analysis of light scattered from plasmas having densities down to $\sim 10^{14}$ cm^{-3} and temperatures up to several hundred electron volts.

I. Introduction

Spectral analysers used in Thomson scattering diagnostics of plasmas have usually been relatively large and expensive owing to their use of conventional photomultiplier tubes as detectors[6,7]. We describe here a four-channel spectral analyser that uses a single interference filter as the dispersive element and avalanche photodiodes for light detection, and is therefore inexpensive and physically compact. It is suitable for analysis of scattering from plasmas having densities down to about 10^{14} cm^{-3} and temperatures up to several hundred electron volts.

II. Description of Analyser

Light is separated into four channels by passing the incident light repeatedly through a single interference filter at varying angles of incidence. Light incident at a particular angle is transmitted only in the narrow band determined by the filter characteristics, the remainder being reflected. This follows from energy conservation and the non-lossy character of all-dielectric interference filters. The reflected light is turned by a pair of individually adjustable mirrors, and re-directed at the filter at a new angle for the next channel, and so on for succeeding channels.

A schematic view of the analyser is shown in Figure 1. All components are mounted in an aluminium box (620 x 220 x 80 mm). The interference filter, 50 mm diameter, is sandwiched between two 30 mm diameter lenses, each having focal length 160 mm. Light is introduced through a commercially available glass fiber optic bundle 2 mm in diameter, with polished ends. The effective focal ratio of the instrument (f/5.3) is determined by the solid angle subtended by the 30 mm diameter lens at the end of the fiber optic bundle. The bundle itself introduces little additional divergence of the light.

The interference filter transmits a band of wavelengths of approximately 15 Å FWHM, centered at 6937 Å at normal incidence. When the angle of incidence is changed, the passband shifts to the blue, the shift being quadratic with angle (Fig. 2). Owing to this dependence upon angle, it is necessary to render the incident light parallel in transmission, which is the function of the first lens. This lens also re-focusses the reflected portion of the spectrum back at a point on the opposite side of the central axis.

The spectrally narrow transmitted beam is focussed by the second lens onto one of the silicon avalanche photodiode detectors. These diodes (RCA 30902E) have a square sensitive area 0.5 mm on a side and acceptance angle of about 100°. It is this element that determines the light gathering power of the instrument (the etendue, equal to the product of detector area and acceptance solid angle, is a good measure of this power).

The image formed by lens 2 is larger than the detector, and is demagnified by a small (4mm diameter, 4.2mm focal length)lens located just in front of the detector. The diameter of the fiber optic input is determined by the size of the image of the detector's sensitive element created by this lens. On the instrument described here, the demagnification factor is 2.8, so the 2mm diameter fiber bundle used for input gives an image that is slightly larger than the silicon chip. It is possible, of course, to obtain larger detector areas, and arrays can also be produced for special requirements.

The focal lengths of the two lenses adjacent to the filter are selected to be just large enough to make a comfortable separation of the detectors and mirrors, so as to allow for some adjustment of channel separation.

Returning to the input side of the filter, the reflected beam comes to a focus at a point opposite the input. Just before reaching focus, it is turned 90^{o} by a small mirror that reflects it to a second mirror, which again turns it about 90^{o}. The beam is thus re-directed back at the filter, but now from a different angle. The transmitted portion of the spectrum from this beam then passes on to another photodiode, and a second reflected beam returns to another pair of mirrors, and so on.

The mirrors are mounted on small stands having a slotted foot that may be fixed to the floor of the box at any position, using one of a square grid of tapped holes in the floor. Each stand (Fig. 3) supports a 4mm diameter brass rod, at the end of which the 10mm square first-surface

mirror is attached. Angular adjustment is achieved by rotation of this rod in its support, and the mirror may be rotated through a small angle about a horizontal axis by a screw on the end of the rod, for up-down alignment. The detectors are mounted, along with their lenses, in 10mm diameter brass housings that are mounted on support stands identical to those used for the mirrors (Fig. 4).

III. Detectors

Silicon avalanche diodes (RCA 30902E) were chosen as detectors because of their small size, which made the compact design possible, and their high sensitivity and low cost. These diodes have high quantum efficiency in the red ($\sim$65% at the 6943Å ruby wavelength), which makes them attractive as detectors for low light levels where quantum statistical noise is a problem. They have internal gain (through avalanche multiplication of the photoelectrons) up to several hundred, adjustable by the reverse bias voltage.

Operating at the manufacturers specification of gain equal to 150, the diode noise is about 2×10^{-13} Amp/Hz$^{\frac{1}{2}}$, low enough so that the output signal-to-noise ratio is determined by the quantum statistics of the photoelectrons for all but exceedingly low light levels. A discussion of the noise characteristics of avalanche diodes is beyond the scope of this paper, and the reader is referred to several articles in the literature[1,2,3,4]. Figure 5 shows the signal-to-noise ratio calculated

for one of these diodes using manufacturer's specifications, as a function of incident light power P. The diode noise goes as P, while quantum noise scales as $P^{\frac{1}{2}}$, at fixed bandwidth. Shown for comparison is the theoretical noise characteristic of a photomultiplier tube assuming the noise here is purely due to photon statistics. In the region where both devices are limited by photon statistics, the diode has better characteristics due to its higher quantum efficiency. The crossover in this case is at an input power of $\simeq 10^{-10}$ watts, corresponding to a pulse of about 10 photons in 30 nanoseconds, the width of a typical laser pulse.

The noise current of the diode is a strong function of the gain, varying approximately as the cube of gain[1], which itself is a very strong function of reverse bias voltage. The noise rises precipitously as the voltage nears the "breakdown" voltage. This is a non-destructive breakdown, that may be exceeded at least briefly if the diode current is sufficiently limited. "Second breakdown" which is destructive, is discussed by Egawa[8].

The principal practical disadvantage of these photodiodes is their strong sensitivity to temperature. Operating at gain around 150, the gain may change between 5 and 10% for a one degree change in temperature, and this sensitivity is worse at higher gain. It would be advisable therefore, to build in temperature control when using them.

In the present instrument, temperature control was not included, and it was necessary to check and adjust gain often. Reverse bias voltage was supplied by a well-regulated power supply with potentiometers being used to trim the bias of individual diodes to equalize their sensitivity. It was found useful to install both coarse and fine voltage adjustments, since trimming adjustments were sensitive to changes of 0.1 Volt at a bias of 220V.

IV. Premaplifier and Output Level

The avalanche photodiodes are current sources, and it is advantageous to arrange for each to see a relatively high impedance level, or to couple it directly to a transimpedance amplifier (current in, voltage out)[5]. We used a commercial hybrid preamplifier (LeCroy VV100B) which has input impedance Z = 17 kΩ, gain G = 10, and risetime of 2 nsec. The overall voltage responsivity R_v of the system is then

$$R_v = RZG \quad ,$$

where R is the current responsivity. For this system, R ≃ 65 Amp/Watt (which includes the avalanche gain), Z = 17 kΩ, and G = 10, so $R_v \simeq 11$ volt/μwatt. A 50 mV output pulse corresponds to about 450 photons incident upon the detector in 30 nsec.

V. Filter

The interference filter serves to isolate the four narrow spectral bands to be recorded. Since the operation of the instrument depends upon utilizing light that has undergone several reflections from the filter, there are stronger constraints upon its construction than are usual for transmission interference filters. The shape of the transmission band must not be unduly modified for angles of incidence up to about 20^{o}, and the reflection spectrum must be the compliment of the transmission spectrum over this range of angles. These characteristics were met in the Baird-Atomic filter used here. It had, however, one undesirable characteristic that could have been avoided had the problem been forseen. It is a filter utilizing two Fabry-Perot interference sandwiches in series, and these were placed on opposite sides of the ∿8mm thick dye glass absorption filter used as a substrate and for sideband suppression. The separation of the reflecting films introduced undesired losses with high angles of incidence. The specification should require all dielectric films to be on one side of the dye glass substrate. It is also desirable to use well-corrected lenses to avoid losses from defocussing by spherical and off-axis aberations.

VI. Alignment

The optical system is aligned in two stages. First the input and several reflected beams on the input side of the filter are aligned using a white light source; and then the detectors are positioned properly. The fiber

optic input is positioned at the largest angle of incidence to be used, and a strong white light source introduced at the other end. The image of the fiber bundle end may be easily located with a small target of white paper, and the first mirror is fixed just in front of this position, oriented to reflect the beam toward the axis. A second mirror is then placed to reflect the beam back at the filter, and located along the proper radial line to give the next largest angle of incidence desired. The orientation of this second mirror is then adjusted so that when one looks from the detector side through the filter (with aid of a small mirror), the spot of red light transmitted may be seen to come from all parts of the filter. This insures that there will be no unnecessary vignetting of the transmitted beam. The process is then repeated for the two other channels.

The diodes are located at the optimum position by looking at their output, when a chopped white light source is introduced as the input. A caution to be observed here : owing to the high sensitivity of the photodiodes to temperature, it will be found that their responsivity drops quickly as the housings are handled during alignment. It is recommended to handle them only by their support bases, and perhaps to wear cotton gloves as well.

Finally the channel widths and positions may be checked with aid of light introduced through a calibrated monochromator. This generally requires a very bright white light source and chopper. Figure 6 shows the result.

VII. Calibration and Drift Suppression

Since a temperature-controlled environment was not provided for this instrument, it was necessary to periodically monitor the gain of the various channels, and to make appropriate adjustments. A small self-contained chopped white light source was constructed for this purpose, using a 6 volt flashlight bulb supplied by a regulated 5V power supply and a chopper driven by a 3 volt toy motor. The fiber optic could be unplugged from the plasma device, and plugged into the light source for a periodic check. The bias voltages were then adjusted to give a standard output signal for all channels. It was determined that it was not necessary to perform this check with a red source.

Such an adjustment is useful as a quick and reproduceable way to establish a standard gain setting. It is not sufficient, however, to establish the true relative gain of the four channels. Small differences in stray capacitance cause the channel sensitivities to show some frequency dependence, so the final gain calibration was done with a pulsed spark source that produced a continuum in a pulse comparable in shape to that of the laser. This calibration was done with the input to the fiber bundle duplicating the optical characteristics of the scattering optics, so that any small sensitivity to divergence of incident light was eliminated.

This work was supported by the Swiss National Science Foundation.

Figure Captions

1. Schematic diagram of the analyser.

2. Shift of passband center as a function of angle of incidence for a typical interference filter.

3. Mirror support stand and mirror mount. The uppermost screw adjusts the mirror about a horizontal axis, and the collar makes possible adjustment about a vertical axis without vertical translation.

4. Photodiode housing with lens.

5. Signal-to-noise ratio for avalanche photodiode (RCA 30902E) (solid line) compared to that of multiplier phototube (RCA 7265).

6. Superimposed transmission characteristics of the four channels.

References

1. R.J. McIntyre, IEEE Trans. on Electron Devices, ED-13, 164 (1966)

2. R.B. Emmons and G. Lucovsky, IEEE Trans. on Electron Devices, ED-13, 297 (1966)

3. K.M. Van Vliet, Appl. Opt. 6, 1145 (1967)

4. R.D. Baertsch, IEEE Trans. on Electron Devices, ED-13, 987 (1966); 383 (1966)

5. R.H. Hamstra and P. Wendland, Appl. Opt. 11, 1539 (1972)

6. A.W. DeSilva and G. Goldenbaum, in Methods of Experimental Physics, Vol. 9B, ed. by Griem and Lovberg (Academic Press, 1971)

7. H.J. Kunze, in Plasma Diagnostics, ed. Lochte-Holtgreven (North Holland Publishing Co., 1968)

8. H. Egawa, IEEE Transactions on Electron Devices, ED-13, 754 (1966).

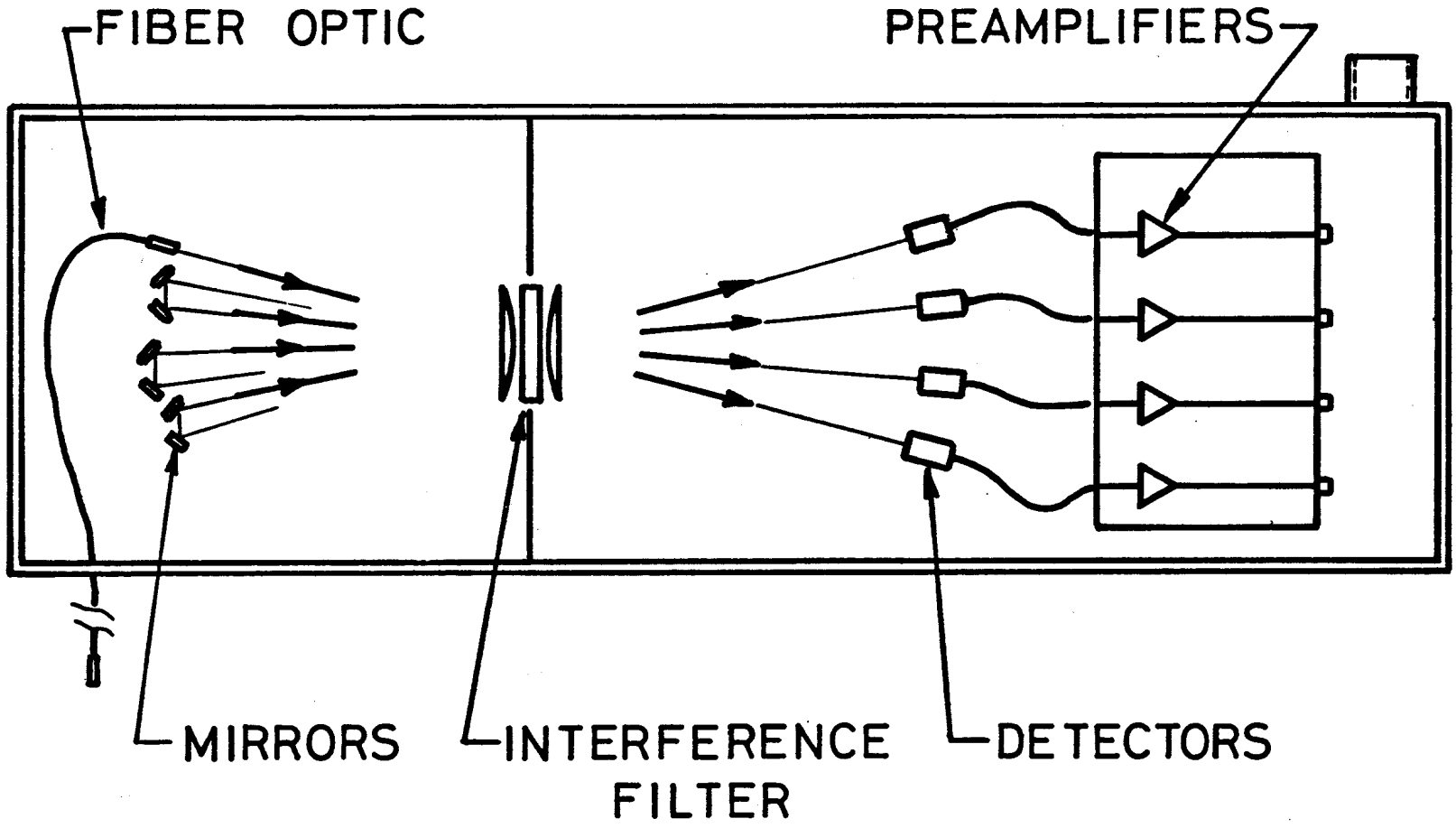
FIBER OPTIC
PREAMPLIFIERS
MIRRORS
INTERFERENCE FILTER
DETECTORS

FIG.1

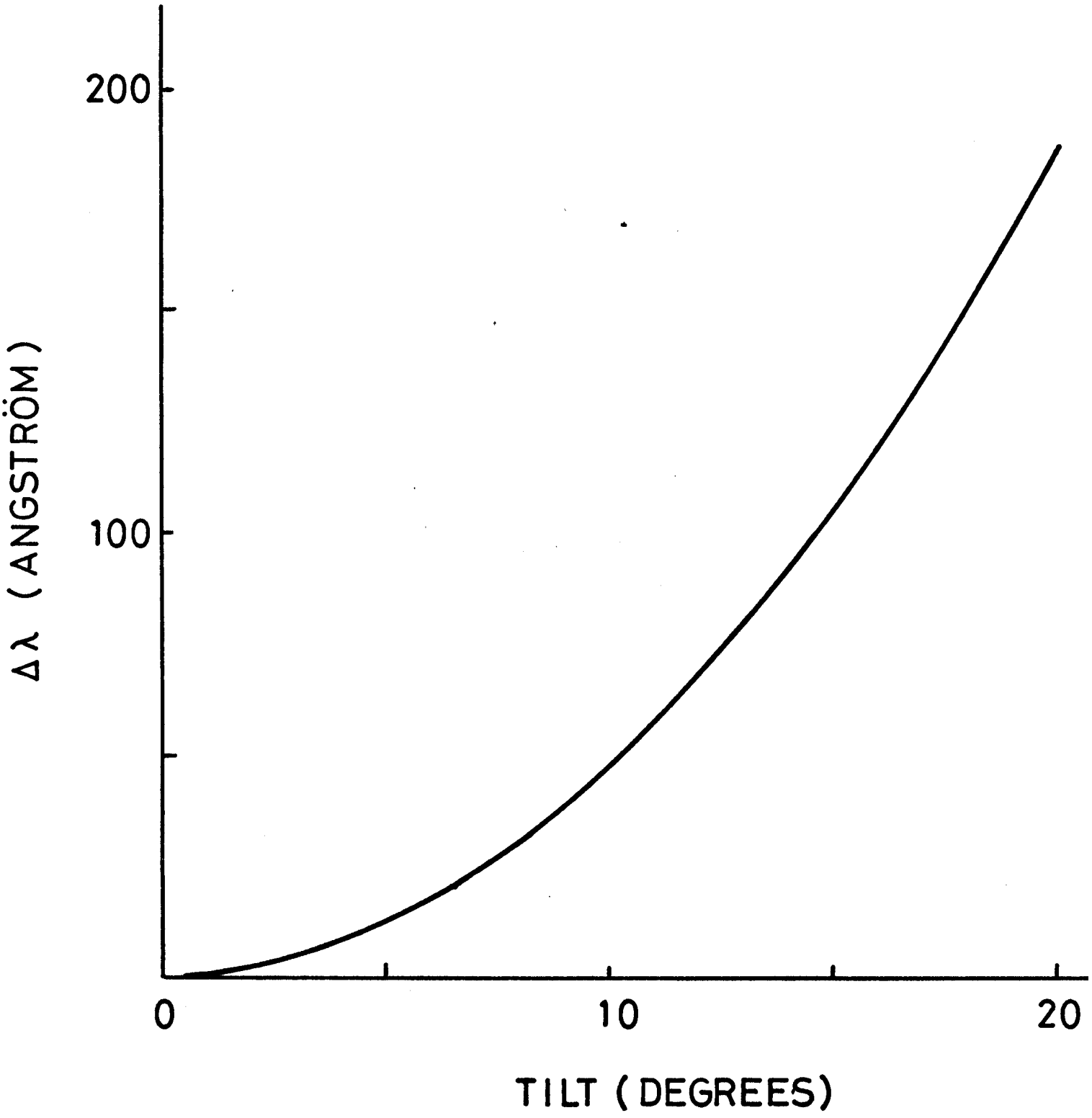

FIG. 2

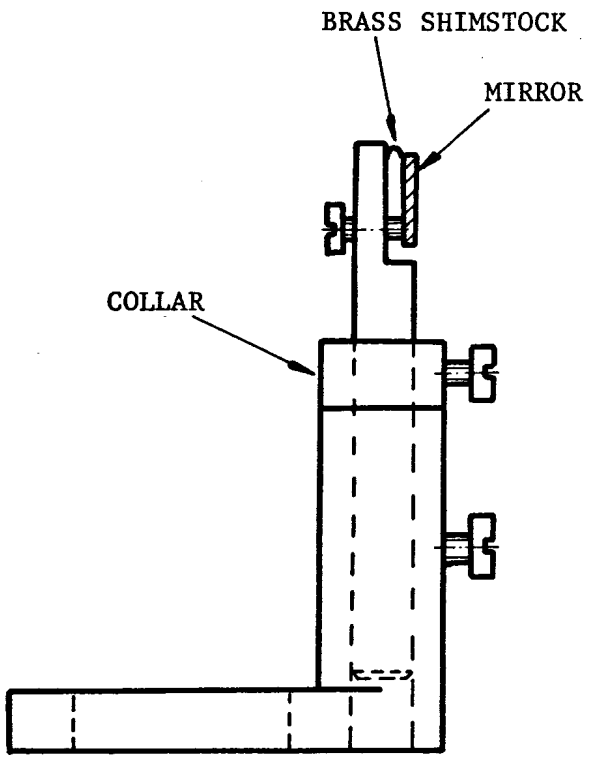

FIG. 3 MIRROR SUPPORT

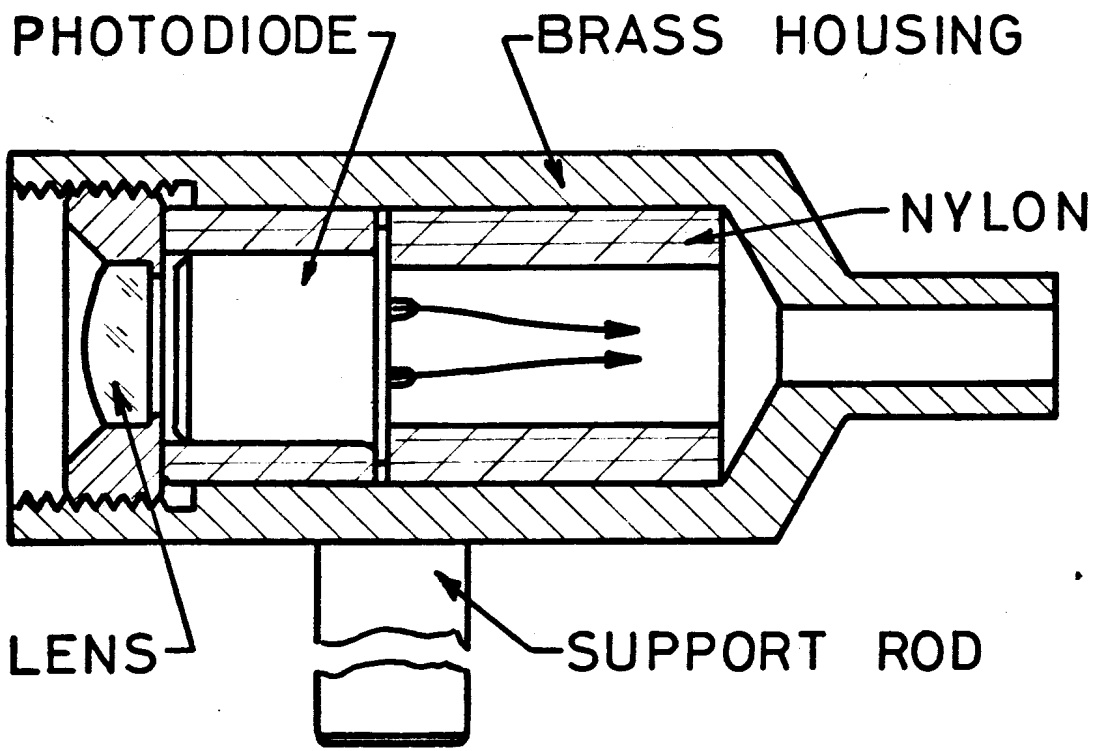

FIG. 4

FIG. 5

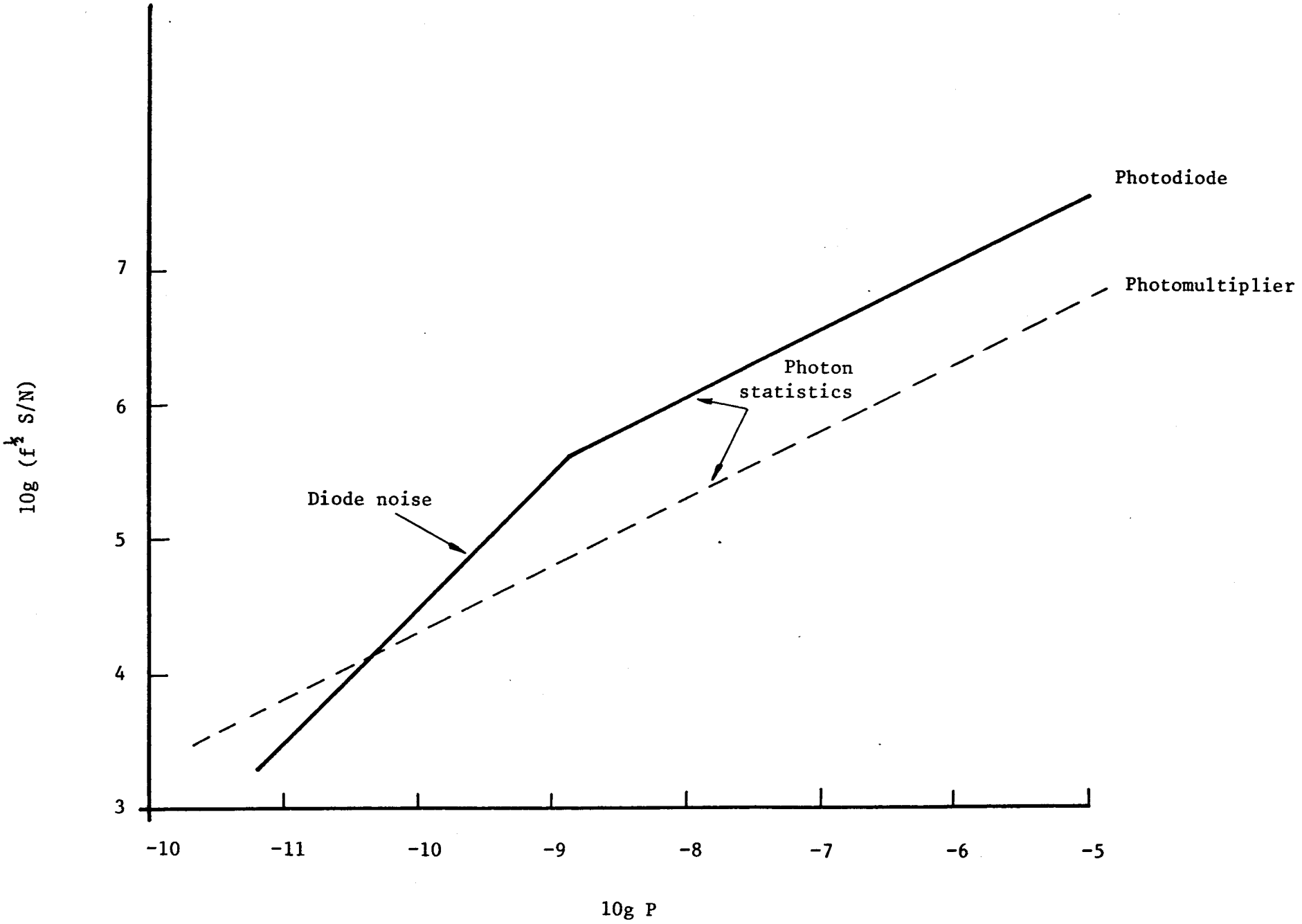
Photodiode
Photomultiplier
Photon
statistics
Diode noise
7
6
5
4
3
10g ($f^{\frac{1}{2}}$ S/N)
-10
-11
-10
-9
-8
-7
-6
-5
10g P

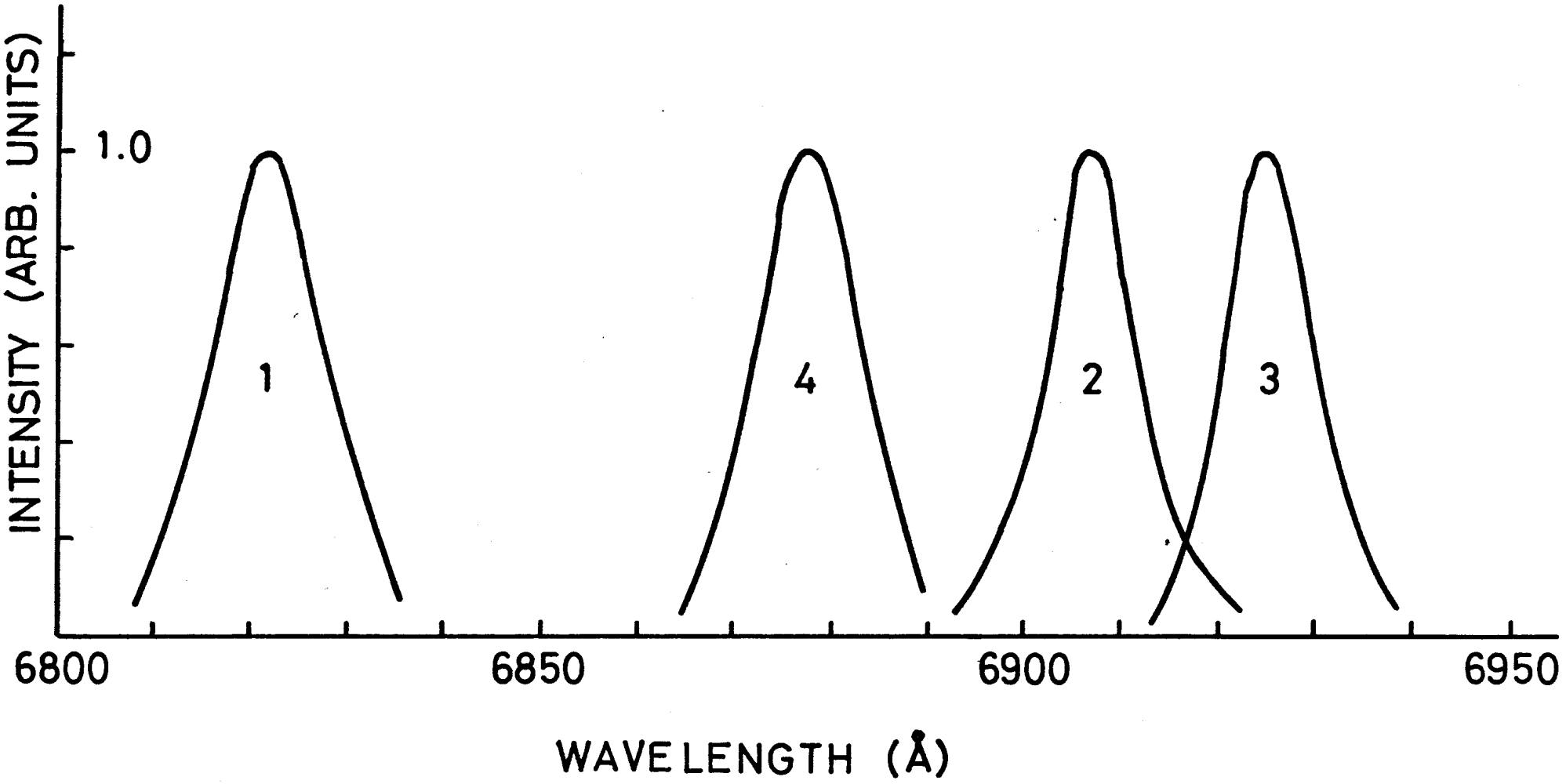
INTENSITY (ARB. UNITS)
1.0
1
4
2
3
6800
6850
6900
6950
WAVELENGTH (Å)

FIG. 6